

Published in final edited form as:

Nat Genet. 2014 April ; 46(4): 376–379. doi:10.1038/ng.2921.

## Recurrent *PTPRB* and *PLCG1* mutations in angiosarcoma

Sam Behjati<sup>#1,2</sup>, Patrick S Tarpey<sup>#1</sup>, Helen Sheldon<sup>#3</sup>, Inigo Martincorena<sup>1</sup>, Peter Van Loo<sup>1,4</sup>, Gunes Gundem<sup>1</sup>, David C Wedge<sup>1</sup>, Manasa Ramakrishna<sup>1</sup>, Susanna L Cooke<sup>1</sup>, Nischalan Pillay<sup>5,6</sup>, Hans Kristian M Vollan<sup>1,7,8</sup>, Elli Papaemmanuil<sup>1</sup>, Hans Koss<sup>9,10</sup>, Tom D Bunney<sup>9</sup>, Claire Hardy<sup>1</sup>, Olivia R Joseph<sup>1</sup>, Sancha Martin<sup>1</sup>, Laura Mudie<sup>1</sup>, Adam Butler<sup>1</sup>, Jon W Teague<sup>1</sup>, Meena Patil<sup>11</sup>, Graham Steers<sup>11</sup>, Yu Cao<sup>12</sup>, Curtis Gumbs<sup>12</sup>, Davis Ingram<sup>12</sup>, Alexander J Lazar<sup>12</sup>, Latasha Little<sup>12</sup>, Harshad Mahadeshwar<sup>12</sup>, Alexei Protopopov<sup>12</sup>, Ghadah A Al Sanna<sup>12</sup>, Sahil Seth<sup>12</sup>, Xingzhi Song<sup>12</sup>, Jiabin Tang<sup>12</sup>, Jianhua Zhang<sup>12</sup>, Vinod Ravi<sup>12</sup>, Keila E Torres<sup>12</sup>, Bhavisha Khatri<sup>5</sup>, Dina Halai<sup>5</sup>, Ioannis Roxanis<sup>11</sup>, Daniel Baumhoer<sup>13</sup>, Roberto Tirabosco<sup>5</sup>, M Fernanda Amary<sup>5</sup>, Chris Boshoff<sup>6,14</sup>, Ultan McDermott<sup>1</sup>, Matilda Katan<sup>9</sup>, Michael R Stratton<sup>1</sup>, P Andrew Futreal<sup>1,12</sup>, Adrienne M Flanagan<sup>5,6</sup>, Adrian Harris<sup>3,11</sup>, and Peter J Campbell<sup>1,15,16</sup>

<sup>1</sup>Cancer Genome Project, Wellcome Trust Sanger Institute, Wellcome Trust Genome Campus, Hinxton, Cambridgeshire, CB10 1SA, UK <sup>2</sup>Department of Paediatrics, University of Cambridge, Hills Road, Cambridge, CB2 2XY, UK <sup>3</sup>The Weatherall Institute of Molecular Medicine, University of Oxford, Oxford, OX3 9DS, UK <sup>4</sup>Human Genome Laboratory, Department of Human Genetics, VIB and KU Leuven, B-3000 Leuven, Belgium <sup>5</sup>Histopathology, Royal National Orthopaedic Hospital NHS Trust, Stanmore, Middlesex, HA7 4LP, UK <sup>6</sup>University College London Cancer Institute, Huntley Street, London, WC1E 6BT, UK <sup>7</sup>Department of Oncology, Oslo University Hospital, N-0310 Oslo, Norway <sup>8</sup>The K.G. Jebsen Center for Breast Cancer Research, University of Oslo, N-0424 Oslo, Norway <sup>9</sup>Institute of Structural and Molecular Biology, Division of Biosciences, University College London, London WC1E 6BT, UK <sup>10</sup>Division of Molecular Structure, MRC-National Institute for Medical Research, Mill Hill, London NW7 1AA, UK <sup>11</sup>Department of Pathology, John Radcliffe Hospital, Oxford, OX3 9DS, UK <sup>12</sup>M. D. Anderson Cancer Center, The University of Texas, 1901 East Road, Houston, Texas 77054, USA <sup>13</sup>Bone Tumour Reference Centre, Institute of Pathology, University Hospital Basel, Basel, Institute for Applied Cancer Science, Switzerland <sup>14</sup>Pfizer Oncology, 10555 Science Center Dr, La Jolla, CA,

Users may view, print, copy, and download text and data-mine the content in such documents, for the purposes of academic research, subject always to the full Conditions of use:[http://www.nature.com/authors/editorial\\_policies/license.html#terms](http://www.nature.com/authors/editorial_policies/license.html#terms)

Correspondence should be addressed to P.C. (pc8@sanger.ac.uk).

### Author contributions

S.B. and P.S.T. performed analyses of sequencing data. H.S. performed *in vitro* experiments. P.V.L. performed copy number analysis. D.C.W. and I.M. performed statistical analyses. S.L.C. performed rearrangement analysis. G.G., N.P., M.R., H.K.M.V., and E.P. contributed to data analysis. H.K., T.B., M.K. contributed structural analyses. C.H., O.J., L.M., H.M., A.P., Ji.T., L.L., Y.C., C.G. coordinated sample processing and technical investigations. Sa.M. coordinated sample acquisition. A.B., J.T., S.S., X.S., J.Z. coordinated informatics analyses. B.K., D.H., D.B., M.P., G.S., I.R., R.T., M.F.A., A.M.F., C.B., V.R., K.E.T., D.L., A.J.L., G.S. and A.H. provided samples and clinical data. P.C., M.R.S., A.H., P.A.F., U.M. and A.M.F. directed the research. M.R.S., P.C., S.B. and P.S.T. wrote the manuscript, with contributions from A.H., A.M.F. and P.A.F.

### Accession codes

Sequencing data have been deposited at the European Genome-Phenome Archive (EGA, <http://www.ebi.ac.uk/ega/>), which is hosted by the European Bioinformatics Institute (EBI); EGAD00001000735.

### Competing financial interests

The authors declare no competing financial interests.

92121 <sup>15</sup>Department of Haematology, Addenbrooke's Hospital, Cambridge, UK <sup>16</sup>Department of Haematology, University of Cambridge, Hills Road, Cambridge, CB2 2XY, UK

# These authors contributed equally to this work.

## Abstract

Angiosarcoma is an aggressive malignancy that arises spontaneously or secondarily to ionising radiation or chronic lymphoedema<sup>1</sup>. Previous work has identified aberrant angiogenesis, including occasional somatic mutations in angiogenesis signalling genes, as a key driver of angiosarcoma<sup>1</sup>. Here, we employed whole genome, exome, and targeted sequencing to study the somatic changes underpinning primary and secondary angiosarcoma. We identified recurrent mutations in two genes, *PTPRB* and *PLCG1*, which are intimately linked to angiogenesis. The endothelial phosphatase *PTPRB*, a negative regulator of vascular growth factor tyrosine kinases, harboured predominantly truncating mutations in 10/39 (26%) tumours. *PLCG1*, a signal transducer of tyrosine kinases, presented with a recurrent, likely activating R707Q missense variant in 3/34 cases (9%). Overall, 15/39 (38%) tumours harboured at least one driver mutation in angiogenesis signalling genes. Our findings inform and reinforce current therapeutic efforts to target angiogenesis signalling in angiosarcoma.

---

We performed whole genome sequencing of three angiosarcomas, along with paired normal DNA from the same patients. The somatic mutation burden of the three cases varied from 0.7–2.2 substitutions per megabase and 0.1–0.2 indels per megabase (Supplementary Fig. 1; Supplementary Table 1-5). Remarkably, in two of the three angiosarcomas we identified truncating mutations in the *PTPRB* (*VE-PTP*) gene, a tyrosine phosphatase specific to vascular endothelium that inhibits angiogenesis<sup>2</sup>. One tumour had a nonsense substitution (p.E1444\*) and the other both a nonsense (p.C1693\*) and a missense (p.Y309C) mutation.

To explore this observation further, we extended our investigation to 36 angiosarcomas which we studied by whole exome sequencing (n=8) or by targeted sequencing of 360 cancer genes (n=4; Supplementary Table 6) or 28 angiogenesis-related genes (n=24; Supplementary Table 7). The entire footprint of *PTPRB* was sequenced, to enable the identification of structural rearrangements in addition to coding point mutations. Angiogenesis-related genes were also sequenced in eight epithelioid haemangi endotheliomas, nine Kaposi's sarcomas, and two haemangiomas.

In total, we identified 14 *PTPRB* mutations in 10/39 (26%) angiosarcomas, comprising eight nonsense, two essential splice, a frameshift insertion and three missense variants (Fig. 1). No large deletions or rearrangements were identified, although the presence of small intragenic deletions cannot be excluded. All truncating mutations disrupt the coding sequence of *PTPRB* before or within the tyrosine phosphatase domain. Two of the missense mutations (Y309C and W130R) lie within the extracellular domain of *PTPRB*, inhibition of which has been shown to disrupt *PTPRB* function<sup>3</sup>. The third missense mutation, P1996L, lies within the tyrosine phosphatase domain. The *in silico* variant effect prediction tool, SIFT, ascribes deleterious consequences to these missense variants. No *PTPRB* mutations were identified

in haemangioendothelioma, Kaposi sarcoma, or in haemangioma. Inactivating *PTPRB* mutations are also rare in other cancer types, as documented in COSMIC<sup>4</sup>, suggesting that *PTPRB* disruption is largely specific to angiosarcoma. Statistical analysis demonstrated that these truncating *PTPRB* mutations were extremely unlikely to have accumulated by chance in angiosarcoma ( $q = 10^{-9}$ ), suggesting that inactivating *PTPRB* mutations are driver events. Notably, all *PTPRB* mutations were identified in tumours that were either known to be secondary and / or have *MYC* amplification, a biomarker of radiation-associated secondary angiosarcoma<sup>5</sup> ( $p = 0.005$ ). In this group the prevalence of *PTPRB* mutations was 45% (10/22 cases).

Four angiosarcomas harboured two different non-synonymous *PTPRB* mutations each, including at least one truncating variant in each case. In two of these cases both mutations were truncating, consistent with biallelic inactivation, suggesting that *PTPRB* operates as a recessive cancer gene. In six angiosarcomas there was a single heterozygous *PTPRB* variant, 5 truncating and one missense, without evidence of LOH. The presence of a single detectable non-synonymous mutation in 60% of tumours is not unusual for tumour suppressor genes (Supplementary Fig. 2). We analysed published catalogues of somatic mutation from 4,073 tumours to determine the frequency of a second mutation, including LOH, co-occurring with a truncating mutation in established suppressor genes. This analysis indicates that the pattern of mutation we observed in *PTPRB* is compatible with a recessive driver mechanism (Supplementary Fig. 2). Nevertheless, we cannot exclude the possibility that other mechanisms such as haploinsufficiency or dominant negative effects are operative.

*PTPRB*, a negative regulator of angiogenesis, is expressed exclusively in vascular endothelium, both during development and in adult tissues<sup>2,6</sup>. It inhibits VEGFR2, VE-cadherin, and angiopoietin signalling, thus acting as an integral modifier of angiogenesis<sup>2,3,6-15</sup>. In *in vitro* models of angiogenesis, *PTPRB* inhibition increases angiogenesis<sup>12</sup>. *PTPRB* null mice die *in utero* and display severe vascular malformations<sup>6</sup>. Although the role of *PTPRB* as a negative regulator of angiogenesis is well established, it is not known whether *PTPRB* driven angiogenesis can be inhibited through pharmacological VEGF inhibition. Consequently, we investigated the effects of knockdown of *PTPRB* on primary cultures of human umbilical vein endothelial cells (HUVEC). Silencing of *PTPRB* via siRNA induced features of angiogenesis such as spheroid sprouting after 24 hours and spindle-like morphology. In the presence of sunitinib or vatalinib, inhibitors of VEGFR2 kinase, these features were abolished (Figure 2; Supplementary Figure 3). These findings in HUVEC, a model of vascular endothelium, provide a rationale for exploring whether *PTPRB* mutation status correlates with treatment response to anti-angiogenic agents.

To explore the contribution of other genes in angiosarcoma we analysed variant data from 15 angiosarcomas interrogated by whole genome, exome, or cancer gene sequencing (Fig. 3). Cancer genes mutated in more than one tumour included *TP53* (3/15 cases; 20%), *KDM6A* (2/15 cases; 13%), and *MYC* (6/15 cases; 40%). Strikingly, we also identified a recurrent missense variant, R707Q, in *PLCG1*, in 3/15 cases (20%). *PLCG1* encodes phospholipase C gamma 1 (PLC $\gamma$ 1), a tyrosine kinase signal transducer within the phosphoinositide signalling pathway. Statistical analysis showed that the enrichment of

R707Q mutation in angiosarcoma is highly significant ( $q = 0.000002$ ). Capillary sequencing of an additional 15 cases of angiosarcoma indicated that the overall prevalence of R707Q mutations was 9% (3/34 cases). No *PLCG1* mutations were found in any of the other tumour types investigated here. Notably, all three *PLCG1* R707Q mutations co-occurred with *PTPRB* mutations.

The presence of a single recurrent R707Q missense variant suggests that *PLCG1* is activated in angiosarcoma. Arginine 707 lies within the auto-inhibitory cSH2 domain of PLC $\gamma$ 1<sup>16-19</sup> and provides structural support to this domain. *In silico* modelling of the mutated protein predicts that the substituted glutamine destabilises the cSH2 domain which may result in overactive PLC $\gamma$ 1 (Supplementary Fig. 4). Disruption of the auto-inhibitory cSH2 domain has been shown to cause murine and human immune disorders through constitutive activation of PLC $\gamma$  enzymes<sup>16-19</sup>. Interestingly, forward genetic screening of zebrafish has identified *PLCG1* as a non-redundant regulator of arterial angiogenesis that transduces activation of VEGF signalling<sup>20,21</sup>, and *Plcg1*-deficient mice exhibit reduced vasculogenesis<sup>22</sup>. *PLCG1* is ubiquitously expressed in normal tissue<sup>17,19</sup>, and whole RNA sequencing of four angiosarcomas, including two positive for *PLCG1* R707Q, demonstrated *PLCG1* expression in each case. In the context of existing knowledge about *PLCG1*, our observations therefore lend support to the hypothesis that activated *PLCG1* drives angiosarcoma, downstream of receptor tyrosine kinases, through constitutive activation of angiogenesis signalling. The effects of *PLCG1* mutations on the response to therapeutics targeting tyrosine kinases will be an important future investigation.

In addition to 15 angiosarcomas screened for driver mutations, we performed a focused screen for mutations in angiogenesis-related genes (Supplementary Table 6) in a further 24 angiosarcomas. Considering both cohorts together, 15/39 angiosarcomas harbour at least one mutation in an angiogenesis-related gene highlighting aberrant angiogenesis as a common driver in a subset of tumours. Mutated genes included *H/K/N-RAS* (5/39 cases), *PIK3CA* (1/39 cases), and *FLT4* (1/39 cases). We did not find variants in *VEGFR2* (*KDR*) that have previously been reported<sup>23</sup> (Supplementary Table 1). Amongst other vascular tumours we identified one Kaposi sarcoma (n=9) with a *PIK3CA* and one epithelioid haemangioendothelioma (n=8) with a *PTEN* driver mutation (Supplementary Table 1). Interestingly, in our series aberrant angiogenesis was most frequent amongst secondary and/or *MYC*-amplified angiosarcomas (12/22 cases), although this observation requires investigation in larger series. There was no evidence of mutual exclusivity of mutations in angiogenesis-related genes (Fig. 3; Supplementary Table 1). In four angiosarcomas we found more than one angiogenesis-related gene mutated, indicating that targeting treatment exclusively at the tyrosine kinase level may not suffice to overcome aberrant angiogenesis.

As angiosarcoma is a rare tumour, combined efforts to curate larger patient series are required to explore further the somatic changes that underpin its pathogenesis. This study, however, provides a first comprehensive insight into the somatic variation in angiosarcoma and identifies frequent mutations in angiogenesis-related genes in a subset of tumours. The next challenge will be to functionally explore these findings in appropriate angiosarcoma models that accommodate the complexity of the driver landscape we report here. It is now

indicated to determine the clinical utility of *PTPRB* and *PLCG1* as possible biomarkers of secondary disease and as novel therapeutic targets in angiosarcoma.

## Online methods

### Patient samples

Informed consent was obtained from all subjects and ethical approval obtained from Cambridgeshire 2 Research Ethics Service (reference 09/H0308/165). Collection and use of patient samples were approved by the appropriate institutional review board (IRB) of each institution.

### Whole genome, exome and cancer gene sequencing

DNA was extracted from 11 angiosarcomas as well as matched normal tissue derived from the same individuals. Three cases were whole genome sequenced to an average depth of at least 40× or 30× for tumour and normal DNA, respectively, as previously described<sup>24</sup>. Whole exome sequencing was performed on 8 cases as previously described<sup>25</sup>, and at least 70% of the coding sequence was covered by 30×. DNA extracted from an additional 4 tumours that did not have matched normal tissue DNA were subjected to targeted sequencing of 360 established and putative cancer gene using a custom made bait set (Agilent) for target enrichment (Supplementary Table 7). Paired end sequencing was performed on Illumina Hiseq 2000 or 2500 analysers. Reads were aligned to the reference human genome (NCBI37) by using BWA on default settings<sup>26</sup>. Reads which were unmapped or PCR-derived duplicates were excluded from the analysis.

### Variant detection

The CaVEMan (cancer variants through expectation maximization) algorithm was used to call single nucleotide substitutions<sup>25</sup>. To call insertions and deletions, we used split-read mapping implemented as a modification of the Pindel algorithm<sup>27</sup>. To call rearrangements we applied the BRASS (breakpoint via assembly) algorithm, which identifies rearrangements by grouping discordant read pairs that point to the same breakpoint event<sup>25</sup>. Post-processing filters were applied to the output to improve specificity. Mutations were annotated to Ensembl version 58.

### Variant validation

In whole genome samples, all coding variants as well as randomly selected mutations, in total 508/15292 (3.3%) substitutions and 342/1386 (25%) indels, were experimentally validated by whole exome sequencing or targeted capture with massively parallel sequencing<sup>25</sup>. The overall precision of the catalogue of substitutions and indels was thus determined to be at least 94%. Rearrangements were validated by defining the exact location of the breakpoint at nucleotide resolution through extraction of split reads across the breakpoint, algorithmically or previously<sup>25</sup>. Variants called in whole exome samples were confirmed by visual inspection or resequencing.

### Angiogenesis gene screen

43 tumours were included in this screen: 24 angiosarcomas; 9 Kaposi's sarcomas; 8 haemangioendotheliomas; 2 haemangiomas. Genes of interest (Supplementary Table 6) and genotyping SNPs were enriched through targeted capture and sequenced by massively parallel sequencing, as described before<sup>25</sup>. The *PLCG1* R707Q mutation was screened for by capillary sequencing (primer sequences available on request).

### RNA sequencing and analysis

Total RNA was isolated from fresh frozen tissue of 4 angiosarcomas using trizol. Standard Illumina RNA libraries of poly-A selected RNA were sequenced on an Illumina HiSeq 2000 (paired end, 75 base pair read length). TopHat<sup>28</sup> (version 1.3.3) was used for alignment. Expression values were derived using Cufflinks<sup>29</sup> (version 1.0.2).

### Detection of copy number variation

Copy number data were derived from whole genome or exome reads using the ASCAT algorithm (version 2.2) and validated by SNP6.0 in 2 cases<sup>30</sup>. In the whole exome extension study, amplifications were derived by comparing the coverage in candidate genes against average coverage across the exome, after normalization using matched germline exome sequencing data. A 1.75-fold increase (corresponding to  $\geq 5$  copies in 50% tumour cells) was reported as an amplification. In the targeted extension study, amplifications were derived by comparing the coverage in candidate genes against the coverage in 96 SNPs of the same sample, both normalised against data from a panel of non-tumour samples. A fivefold increase in relative, normalised coverage in tumours was reported as an amplification. To assess LOH in *PTPRB*, all SNPs that lie within the footprint of the gene were interrogated and their allele fraction assessed for deviations from 0.5.

### Cell culture

Human Umbilical Vein Endothelial Cells (HUVEC) pooled from multiple donors were purchased from Lonza (Wokingham, UK). These were routinely cultured in Endothelial Growth Medium 2 (EGM-2) (Lonza) up to passage 7 and cultured in Endothelial Basal Medium 2 (EBM-2) (Lonza) during the experiments.

### RNAi transfection

Stealth siRNAs targeting *PTPRB* (HSS108847 and HSS108849) and the Stealth RNAi<sup>TM</sup> siRNA Negative Control Med GC Duplex #2 were purchased from Life Technologies. siRNA was transfected into HUVEC at a final concentration of 30nM using Lipofectamine RNAiMAX reagent (Life Technologies). Cells were transfected at 50% confluency in Opti-MEM reduced Serum Medium with Glutamax 1 (Life Technologies) and used after 24 hours.

### Western blotting and staining

Antibodies for western blotting were obtained from the following suppliers; anti-b-actin HRP (Sigma), anti-VEGFR2 and anti-P-VEGFR2 (Cell Signalling). Staining was performed

on formalin fixed cells using anti-VE-cadherin (Cell Signalling) and Alexa Fluor 488 (Life Technologies).

### Hanging drop assay

HUVEC were trypsinised and resuspended in EBM2 (Lonza) containing 2% foetal calf serum (FCS) at a concentration of  $2.5 \times 10^4$  cells/ml. Methylcellulose was added at 0.25% (w/v) and 20 $\mu$ l drops were seeded in non-adherent dish. After inversion of the plate, suspended cells form a single spheroid containing approximately 500 cells. Treated spheroids were incubated with 1 $\mu$ M Sunitinib (Cell Signaling Technology, Inc) or 100nM Vatalanib (Santa Cruz) for 1hr prior to being embedded in a fibrin gel using 2.5mg/ml fibrinogen-PBS solution (Sigma) and 0.007 units of thrombin (Sigma). Once clotting occurred, EBM-2 containing 2% FCS was added with or without 1 $\mu$ M Sunitinib or 100nM Vatalanib. Spheroid photographs were taken after 24 hours using an AMG Evos XL Core digital microscope (Fisher Scientific, Loughborough, UK). Sprouting area was measured using ImageJ64 software and the results were analysed using Graphpad Prism version 6 (Graphpad Software).

### Statistical analyses

A Fisher's exact test was used to assess the significance of the association between *PTPRB* mutations and subtypes of angiosarcoma.

For analysis of *in vitro* findings, a one-way ANOVA was performed on the data with a Sidak's multiple comparisons test.

To determine whether the frequency of individual mutations classes was higher than expected by chance for each gene, we implemented a likelihood model as previously described<sup>31</sup>. To determine the probability of the identical *PLCG1* mutations having occurred by chance, we used the following approach: Using the rates of each mutation class estimated using the aforementioned method, the neutral rate of such an event assuming uniform mutation rates was determined to be 5.905e-06. The probability of seeing this site mutated three times in the coding sequence of 11 samples that were interrogated by unbiased sequencing was therefore approximately 4.57e-14 (cumulative Poisson distribution). Adjusting the p-value for the total number of sites in the exome the q-value for this mutation is 1.49e-06.

In order to analyse the frequency of two-hits in known tumour suppressor genes we downloaded publicly available catalogues of somatic mutations including copy number data from 4,073 tumours of the Tumour Cancer Gene Atlas consortium (as of November 2013). For every gene of a list of established tumour suppressors (see Supplementary Figure 2) we selected all those samples in which the gene had a truncating mutation (nonsense, essential splice site or out-of-frame indels) and quantified the frequency of a second mutations, i.e. truncating, loss of heterozygosity, missense, or in-frame indel, in the gene. Error bars in Supplementary Figure 2 indicate the 95% confidence intervals of the total fraction of 2-hit samples (using a Chi-square approximation, as implemented in the function "prop.test" in R version 3.0.1).

## Supplementary Material

Refer to Web version on PubMed Central for supplementary material.

## Acknowledgements

This work was supported by funding from the Wellcome Trust (grant reference 077012/Z/05/Z). The material was obtained from the RNOH Musculoskeletal Research Program and Biobank and the Oxford Radcliffe Biobank. Support was provided to A.M.F. (UCL) by the National Institute for Health Research, UCLH Biomedical Research Centre, and the CRUK UCL Experimental Cancer Medicine Centre. Support was provided to A.H. by Cancer Research UK, Oxford Biomedical Research Centre and the Breast Cancer Research Foundation. P.J.C. is personally funded through a Wellcome Trust Senior Clinical Research Fellowship (grant reference WT088340MA). P.V.L. is a postdoctoral researcher of the Research Foundation - Flanders (FWO). HKMV is supported by the Norwegian Radium Hospital's Foundation. SB is funded through the Wellcome Trust PhD Programme for Clinicians. PAF is supported by the Cancer Prevention Research Institute of Texas and the Welch Foundation. We thank Marian Taylor and Russell Leek for sample preparation. We are grateful to the patients for participating in the research and to the clinicians and support staff involved in their care, from Oxford University Hospitals NHS Trust, the University of Texas MD Anderson Cancer Center Sarcoma Programme, and the London Sarcoma Service.

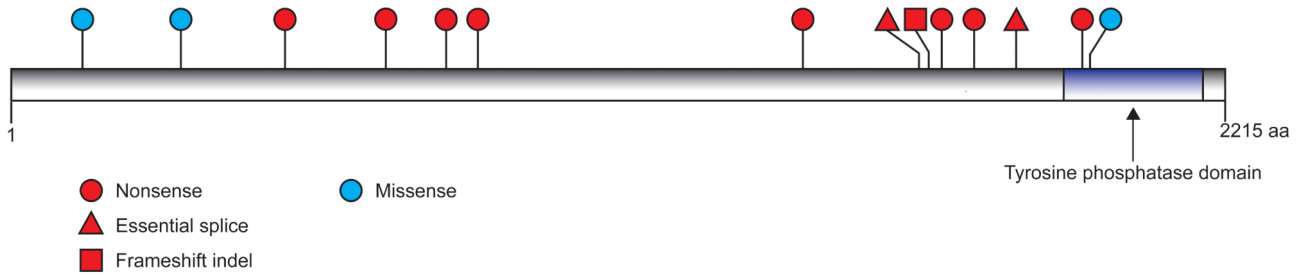
## References

1. Young RJ, Brown NJ, Reed MW, Hughes D, Woll PJ. Angiosarcoma. *Lancet Oncol.* 2010; 11:983–91. [PubMed: 20537949]
2. Fachinger G, Deutsch U, Risau W. Functional interaction of vascular endothelial-protein-tyrosine phosphatase with the angiopoietin receptor Tie-2. *Oncogene.* 1999; 18:5948–53. [PubMed: 10557082]
3. Winderlich M, et al. VE-PTP controls blood vessel development by balancing Tie-2 activity. *J Cell Biol.* 2009; 185:657–71. [PubMed: 19451274]
4. Bamford S, et al. The COSMIC (Catalogue of Somatic Mutations in Cancer) database and website. *Br J Cancer.* 2004; 91:355–8. [PubMed: 15188009]
5. Guo T, et al. Consistent MYC and FLT4 gene amplification in radiation-induced angiosarcoma but not in other radiation-associated atypical vascular lesions. *Genes Chromosomes Cancer.* 2011; 50:25–33. [PubMed: 20949568]
6. Dominguez MG, et al. Vascular endothelial tyrosine phosphatase (VE-PTP)-null mice undergo vasculogenesis but die embryonically because of defects in angiogenesis. *Proc Natl Acad Sci U S A.* 2007; 104:3243–8. [PubMed: 17360632]
7. Baumer S, et al. Vascular endothelial cell-specific phosphotyrosine phosphatase (VE-PTP) activity is required for blood vessel development. *Blood.* 2006; 107:4754–62. [PubMed: 16514057]
8. Broermann A, et al. Dissociation of VE-PTP from VE-cadherin is required for leukocyte extravasation and for VEGF-induced vascular permeability in vivo. *J Exp Med.* 2011; 208:2393–401. [PubMed: 22025303]
9. Carra S, et al. Ve-ptp modulates vascular integrity by promoting adherens junction maturation. *PLoS One.* 2012; 7:e51245. [PubMed: 23251467]
10. Hayashi M, et al. VE-PTP regulates VEGFR2 activity in stalk cells to establish endothelial cell polarity and lumen formation. *Nat Commun.* 2013; 4:1672. [PubMed: 23575676]
11. Li Z, et al. Embryonic stem cell tumor model reveals role of vascular endothelial receptor tyrosine phosphatase in regulating Tie2 pathway in tumor angiogenesis. *Proc Natl Acad Sci U S A.* 2009; 106:22399–404. [PubMed: 20018779]
12. Mellberg S, et al. Transcriptional profiling reveals a critical role for tyrosine phosphatase VE-PTP in regulation of VEGFR2 activity and endothelial cell morphogenesis. *FASEB J.* 2009; 23:1490–502. [PubMed: 19136612]
13. Nawroth R, et al. VE-PTP and VE-cadherin ectodomains interact to facilitate regulation of phosphorylation and cell contacts. *EMBO J.* 2002; 21:4885–95. [PubMed: 12234928]



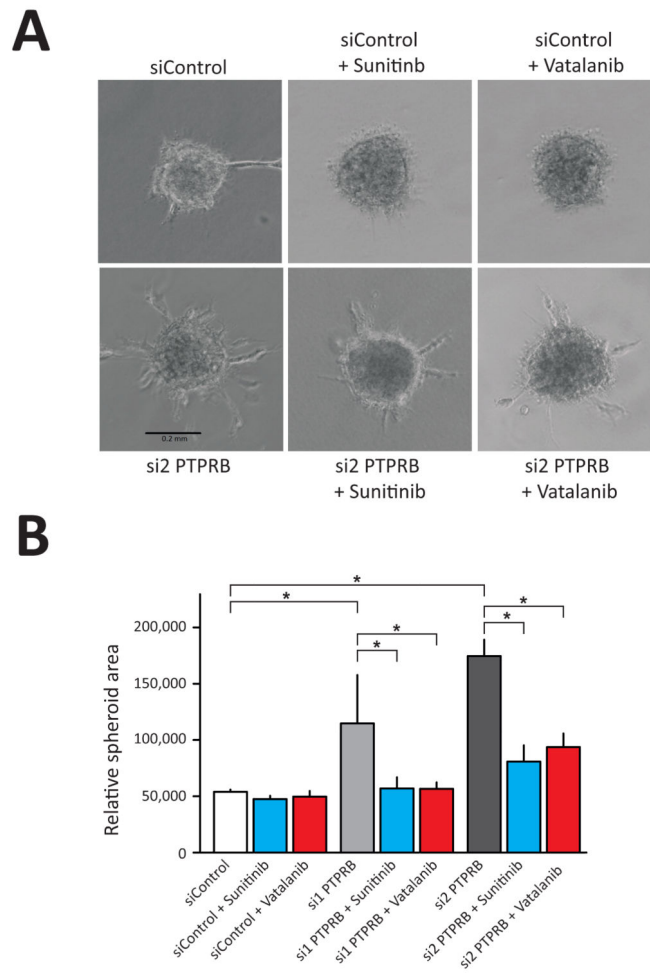
14. Nottebaum AF, et al. VE-PTP maintains the endothelial barrier via plakoglobin and becomes dissociated from VE-cadherin by leukocytes and by VEGF. *J Exp Med*. 2008; 205:2929–45. [PubMed: 19015309]
15. Saharinen P, Eklund L, Pulkki K, Bono P, Alitalo K. VEGF and angiopoietin signaling in tumor angiogenesis and metastasis. *Trends Mol Med*. 2011; 17:347–62. [PubMed: 21481637]
16. Zhou Q, et al. A hypermorphic missense mutation in PLCG2, encoding phospholipase Cgamma2, causes a dominantly inherited autoinflammatory disease with immunodeficiency. *Am J Hum Genet*. 2012; 91:713–20. [PubMed: 23000145]
17. Everett KL, et al. Characterization of phospholipase C gamma enzymes with gain-of-function mutations. *J Biol Chem*. 2009; 284:23083–93. [PubMed: 19531496]
18. Ombrello MJ, et al. Cold urticaria, immunodeficiency, and autoimmunity related to PLCG2 deletions. *N Engl J Med*. 2012; 366:330–8. [PubMed: 22236196]
19. Bunney TD, et al. Structural and functional integration of the PLCgamma interaction domains critical for regulatory mechanisms and signaling deregulation. *Structure*. 2012; 20:2062–75. [PubMed: 23063561]
20. Covassin LD, et al. A genetic screen for vascular mutants in zebrafish reveals dynamic roles for Vegf/Plcg1 signaling during artery development. *Dev Biol*. 2009; 329:212–26. [PubMed: 19269286]
21. Lawson ND, Mugford JW, Diamond BA, Weinstein BM. phospholipase C gamma-1 is required downstream of vascular endothelial growth factor during arterial development. *Genes Dev*. 2003; 17:1346–51. [PubMed: 12782653]
22. Liao HJ, et al. Absence of erythropoiesis and vasculogenesis in Plcg1-deficient mice. *J Biol Chem*. 2002; 277:9335–41. [PubMed: 11744703]
23. Antonescu CR, et al. KDR activating mutations in human angiosarcomas are sensitive to specific kinase inhibitors. *Cancer Res*. 2009; 69:7175–9. [PubMed: 19723655]
24. Behjati S, et al. Distinct H3F3A and H3F3B driver mutations define chondroblastoma and giant cell tumor of bone. *Nat Genet*. 2013; 45:1479–1482. [PubMed: 24162739]
25. Tarpey PS, et al. Frequent mutation of the major cartilage collagen gene COL2A1 in chondrosarcoma. *Nat Genet*. 2013 [PubMed: 23770606]
26. Li H, Durbin R. Fast and accurate long-read alignment with Burrows-Wheeler transform. *Bioinformatics*. 2010; 26:589–95. [PubMed: 20080505]
27. Ye K, Schulz MH, Long Q, Apweiler R, Ning Z. Pindel: a pattern growth approach to detect break points of large deletions and medium sized insertions from paired-end short reads. *Bioinformatics*. 2009; 25:2865–71. [PubMed: 19561018]
28. Trapnell C, Pachter L, Salzberg SL. TopHat: discovering splice junctions with RNA-Seq. *Bioinformatics*. 2009; 25:1105–11. [PubMed: 19289445]
29. Trapnell C, et al. Transcript assembly and quantification by RNA-Seq reveals unannotated transcripts and isoform switching during cell differentiation. *Nat Biotechnol*. 2010; 28:511–5. [PubMed: 20436464]
30. Van Loo P, et al. Allele-specific copy number analysis of tumors. *Proc Natl Acad Sci U S A*. 2010; 107:16910–5. [PubMed: 20837533]
31. Greenman C, Wooster R, Futreal PA, Stratton MR, Easton DF. Statistical analysis of pathogenicity of somatic mutations in cancer. *Genetics*. 2006; 173:2187–98. [PubMed: 16783027]

## PTPRB

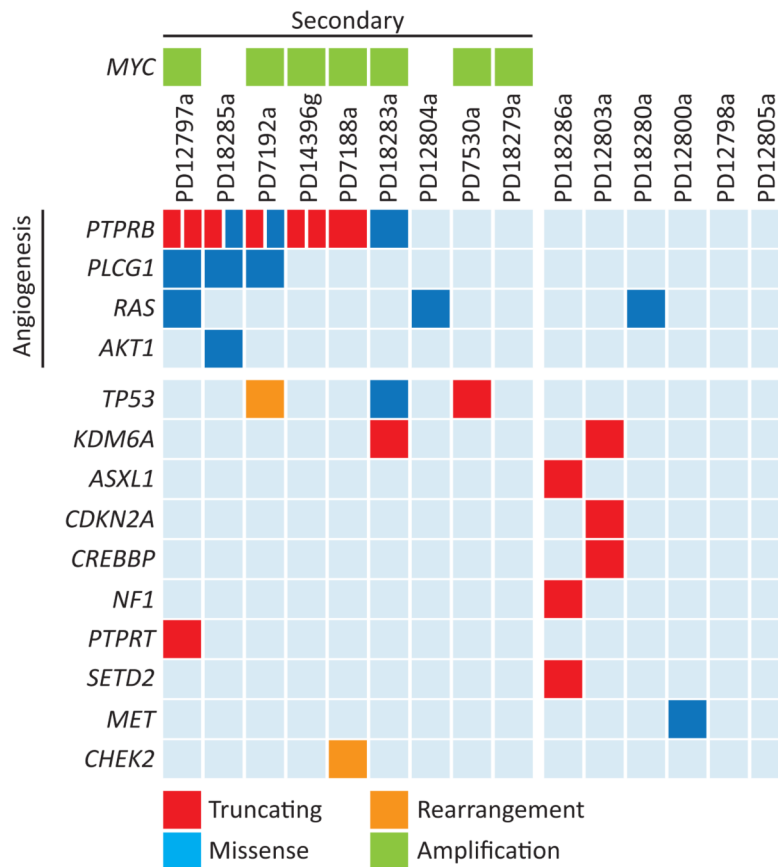
**Figure 1.**

Distribution of mutations in PTPRB.

Each circle / square / triangle represents a mutation. Red: truncating mutations. Blue: missense.



**Figure 2.** Sensitivity of PTPRB-driven angiogenesis to VEGF inhibition. A) HUVEC spheroids embedded in a fibrin gel were photographed after 24 hours of treatment ( $\times 10$  magnification). B) Quantification of spheroid sprouting area. Error bars represent  $1 \times$  standard deviation.  $*p < 0.0001$ .

**Figure 3.**

## Driver variants in angiosarcoma

Likely driver variants are indicated by coloured rectangles. Truncating variants (red) include nonsense, essential splice and frameshift indels. Missense substitutions are indicated in blue, amplifications in green and rearrangements in orange. Secondary angiosarcomas are either clinically classified as secondary or unclassified cases with *MYC* amplification.